Solubility, stability, and bioaccessibility improvement of curcumin encapsulated using 4-α-glucanotransferase-modified rice starch with reversible pH-induced aggregation property

Hye Rin Park[a], Shin-Joung Rho[b],[**],[1], Yong-Ro Kim[a],[b],[c],[*],[1]

[a] Department of Biosystems and Biomaterials Science and Engineering, Seoul National University, Seoul, 08826, Republic of Korea
[b] Center for Food and Bioconvergence, Seoul National University, Seoul, 08826, Republic of Korea
[c] Research Institute of Agriculture and Life Sciences, Seoul National University, Seoul, 08826, Republic of Korea

A B S T R A C T

Curcumin is a polyphenolic compound with anti-cancer, anti-inflammatory and anti-oxidant effects. However, its application in the food industry is very limited owing to its low water solubility and chemical stability. In the present study, 4αGTase-treated rice starch (GS) was prepared by treating rice starch with 4-α-glucanotransferase (4αGTase) for 1 h (1 GS) and 96 h (96 GS), and the physicochemical properties of GS were analyzed. Moreover, the capability of GS to improve the encapsulation efficiency and stability of curcumin by forming complexes was investigated in comparison with maltodextrin (MD) and β-cyclodextrin (CD). GS is known to contain cyclic glucans and amylopectin clusters that contribute to its complex forming capability with bioactive compounds. Upon encapsulation with 1 GS and 96 GS, curcumin solubility increased by 2,241- and 2,846-fold, respectively. UV stability of the encapsulated curcumin with 96 GS also improved by 1.83-fold. GS was effective under all pH conditions except for 96 GS under acidic condition, as well as curcumin encapsulated with 1 GS and 96 GS exhibited 11.53- and 11.27-fold increase in bioaccessibility. The increased stability of curcumin within GS may be attributed to the unique molecular structure of GS interacting with curcumin, as suggested by chromatography and Fourier transform infrared spectroscopy. Also, the improved bioaccessibility of curcumin encapsulated with 96 GS even with lower pH stability at acidic pH seems to be partly attributed to reversible pH-induced aggregation of 96 GS. These results suggest that GS could act as a novel food-grade host material to improve the chemical stability of curcumin.

1. Introduction

Curcumin (bis-α, β-unsaturated β-diketone) is a yellow-orange polyphenol that has been widely used as a natural food colorant with high consumer acceptance. It is derived from the plant *Curcuma longa* (rhizome of turmeric) and is well-known as a potential anti-inflammatory, anti-cancer, anti-microbial, anti-oxidant and anti-mutagenic agent with low toxicity at high doses (Esatbeyoglu et al., 2012). Curcumin has been used as a stabilizer in jelly products and as a natural dye in cheese, pickle, mustard, cereal, soup, ice cream and yogurt (Paramera, Konteles, & Karathanos, 2011). However, the application of curcumin as a food additive has been limited because of its low water solubility (11 ng/mL), stability, and bioavailability (Kaminaga et al., 2003; Kharat, Du, Zhang, & McClements, 2017; Mangolim et al., 2014;

Pan, Zhong, & Baek, 2013; Tonnesen, Masson, & Loftsson, 2002). It is highly unstable under acidic or alkaline pH conditions and can be crystallized or degraded by pH variation. Photodegradation of curcumin also affects its viability in the food system, because curcumin is easily degraded under not only visible light but also ultraviolet (UV) radiation (Lee, Choi, Kim, & Hong, 2013; Tonnensen et al., 2002; Paramera et al., 2011). Moreover, curcumin undergoes rapid first-pass metabolism once it is orally consumed, and almost 90% of curcumin is degraded in the liver and small intestine before entering the systemic circulation (Pan, Huang, & Lin, 1999). Therefore, curcumin must be protected from the physiological environment so that it can be widely used in the food industry (Kharat et al., 2017).

There have been many efforts to improve curcumin stability, water solubility and bioavailability through various encapsulation methods

using nature-derived materials, such as β-cyclodextrin (CD), HP-CD, hydrophobically modified starch (HMS) and yeast (Ansari & Parveen, 2016; Jantarat et al., 2014; Mangolim et al., 2014; Mohan, Sreelakshmi, Muraleedharan, & Joseph, 2012; Paramera et al., 2011; Rachmawati, Edityaningrum, & Mauludin, 2013). However, while the CD production process has been simplified in recent years, it remains a complex process that requires two separate enzyme treatments (cyclodextrin glycosyl transferase and α-amylase) and further purification to remove α- and γ-CDs (Biwer, Aantranikian, & Heinzle, 2002). Also, the low water solubility of CD (1.85% w/v) limits its application in liquid foods (Del Valle, 2004). HMS application is also limited because it is a chemically modified starch treated with *n*-octenyl succinic anhydride (*n*-OSA). Min et al. (2010) reported that the low average molecular weight (Mw) and broad Mw distribution of maltodextrin (MD) limit its usage because host materials with low Mw tend to result in low core material stability in encapsulation systems. Therefore, an easily producible starch material that can achieve robust functionality and stability without chemical treatment is required.

Rice starch is a natural, common and inexpensive source of polysaccharides that has been used as a stabilizer, thickener, binder and fat mimetic in various foods (Clerici & Schmiele, 2019). However, native rice starch is undesirable for use as a wall material because of its low water solubility and irreversible high viscosity at low concentrations after gelatinization or swelling (Fennema, Damodaran, & Parkin, 2017). Hence, many studies have aimed to improve the water solubility of starch through chemical, physical and biological treatment. Specifically, enzymatic treatment of starch has been used to alter its physicochemical properties, such as gelation kinetics, suspension viscosity, water solubility, chain distribution, and Mw distribution. In particular, 4-α-glucanotransferase (EC 2.4.1.25; 4αGTase), a disproportioning enzyme, is known to modify starch structure by transferring α-glucan molecules. 4αGTase attacks α-1,4-glucosidic bonds and transfers α-glucan chains from donor α-glucan molecules to acceptor α-glucans by forming new α-1,4-glucosidic bonds (Cho, Auh, Kim, Ryu, & Park, 2009; Kim, Kim, Trinh, Kim, & Moon, 2012; van der Maarel & Leemhuis, 2013; Park et al., 2007). 4αGTases are classified into five categories: Types 1, 2, 3, 4, and 5. 4αGTase from *Thermus aquaticus* is a Type 2 enzyme, also known as a D-enzyme or amylomaltase (Takaha & Smith, 1999). 4αGTase treatment of starch produces various types of glucans, such as cyclic glucans, linear glucans and highly branched glucans, which may be useful host materials.

Many researchers have studied the physicochemical properties of 4αGTase-treated starch. For instance, thermoreversible gelation (Mun, Choi, Shim, Park, & Kim, 2011), cryoprotection (Kim, Mun, Park, Shim, & Kim, 2013) and gelation kinetics (van der Maarel et al., 2005) were found to be unique characteristics of 4αGTase-treated starch. However, the interaction between 4αGTase-treated starch and hydrophobic bioactive compounds, such as curcumin, has not yet been studied, and nor has the application of 4αGTase-treated starch in encapsulation systems to enhance water solubility, stability and bioaccessibility.

Therefore, we used 4αGTase-treated starch (GS) in a curcumin encapsulation system. We expected GS to be effective in encapsulating bioactive compounds because of its physicochemical properties. The main objective of the present study was to investigate the physicochemical properties of GS treated for 1 h and 96 h and their impacts on the solubility, physicochemical stability and bioaccessibility of curcumin in a water-based chemical-free encapsulation system compared to other starch derivatives (MD and β-CD). We evaluated the interactions between starch and curcumin stability under various pH and UV conditions, and investigated curcumin bioaccessibility using an *in vitro* simulated digestion system.

2. Materials and methods

2.1. Materials

A Korean rice cultivar, *Ilpum* rice was supplied by Rural Development Administration of Korea. Samyang Genex Co. (South Korea) provided maltodextrin (MD, 8–10 Dextrose Equivalent, Avg. Mw = 2,160 Da) that was made from corn starch by partial hydrolysis using α-amylase. The recombinant *Thermus aquaticus* 4-alpha-glucanotranferase (4αGTase) was cloned and expressed in *Eecherichia coli* and purified according to the previous study (Park et al., 2007). Luria-Bertani medium for *E. coli* incubation was purchased from Becton, Dickinson and Company (Sparks, MD, USA). β-cyclodextrin and curcumin with > 94% purity were purchased from Sigma-Aldrich Co. (USA), and cycloamylose (Mw = 8,000 g/mol) was bought from Ezaki Glico Co., LTD. (Japan). HCl and NaOH were from Duksan Pure Chemicals Co. Ltd. (South Korea). Sodium phosphates (monobasic, anhydrous; dibasic, anhydrous) were purchased from Showa Chemical Co. (Japan). Other reagents were bought from Junsei Chemical Co. (Japan) and Duksan Pure Chemicals Co. Ltd. (Kyungki, Korea). All chemicals and reagents used were of analytical grade.

2.2. Preparation of 4αGTase-treated rice starch

4αGTase-treated rice starch (GS) was prepared following the procedure described by Park, Park, and Jane (2007), with minor modification. *Ilpum* rice starch was dispersed in distilled water (50% v/w) and boiled at 95 °C for 30 min with mechanical stirring. Then 4aGTase (20 U/g, dry basis) was added to the cooled pastes with following incubation at 75 °C for 1 h (1 GS) and 96 h (96 GS) with continuous stirring. The reaction was terminated by boiling dispersions at 95 °C for 20 min, and a 5-fold volume of 95% ethanol was added to precipitate the starch. Then, the precipitates separated by centrifugation (9,000 rpm, 20 min) were dried in a dry oven at 40 °C. Dried samples were finely before to use.

2.3. Physicochemical properties of 4αGTase-treated rice starch

2.3.1. Molecular weight distribution (HPSEC)

Starch samples (Maltodextrin (MD), 1 GS, and 96 GS) were dissolved (5% w/v) in 90% DMSO solution and boiled for 30 min. The hot solution was stirred using a magnetic bar for 1 day at room temperature for complete dissolution. Then a 5-fold volume of 95% (v/v) ethanol was added to precipitate the starch. The sediments were washed by adding 2-fold volume of acetone with following centrifugation (12,000 rpm, 10 min), and the washed samples were collected and dried in a dry oven at 45 °C overnight. The dried starch pallets were finely ground using a mortar and 0.5% (w/v) of the starch was dissolved in distilled water with following heating at 95 °C. The sample was injected into a HPSEC (High performance size exclusion chromatography) system after filtering by a 5.0 μm disposable membrane filter. The HPSEC system was composed of two running columns (OH-Pak 804, OH-806 HQ, Shodex), a column, and a refractive index detector (ProStar 355 RI Detector, Varian Inc., Australia). The columns were run at 50 °C and the flow rate of the mobile phase (degassed distilled water) was 0.4 mL/min. Pullulans standards (Shodex Standards, Japan) were used as a molecular weight standard.

2.3.2. Distribution of branched chain length (HPAEC)

Pre-treatment step for HPAEC (High performance anion exchange chromatography) analysis was just same as the step for the HPSEC analysis. Starch solution was prepared by dissolving starch samples (0.5% w/v) in 50 mM sodium acetate (pH 4.5) buffer and boiling for 15 min. To debranch side chain of the starch, 0.2 U/mg of isoamylase was added and incubated for 3 h at 40 °C. The samples were then boiled for 10 min to terminate the enzymatic reaction and filtered using a

0.45 μm membrane filter. HPAEC-PAD (Dionex ICS-3000, Dionex Cor., USA) was equipped with a pulsed amperometry detector (ED40, Dionex) and a column CarboPac TM PA1 was used (4 × 250 mm, Dionex, USA). Two eluents (A, B; 0.150 M sodium hydroxide and 0.15 M sodium hydroxide in 0.6 M sodium acetate solution) were used to equilibrate the system. All measurements were operated at a flow rate of 1 mL/min.

2.3.3. Complex formation capacity

Complex formation capacity of the starch samples was evaluated by an amylose-iodine absorption method with slight modification (Knutson, 1999). The samples were completely dissolved in 90% DMSO solution (0.5% w/v) by mechanical stirring. The solutions were 50-fold diluted with distilled water, and 4 mL of the diluted solution was mixed with 800 μL of iodine solution (0.0025M I_2 and 0.0065M KI). After reacting for 5 min, the absorbance spectra were scanned by UV/Vis spectrophotometer (UV-1650PC, SHIMADZU Co., Japan) from 400 nm to 800 nm.

2.3.4. pH-induced aggregation of 4αGTase-treated rice starch

Change in turbidity and zeta potential of starch suspensions at various pH was evaluated as an index of aggregation, following a method by Perera and Hoover (1999) with modification. MD, 1 GS and 96 GS were mixed (5% (w/v)) with 10 mM phosphate buffer solution (pH 7) and heated for 30 min at 95 °C with mechanical stirring. After the suspensions were cooled at room temperature, 1 N HCl or 1 N NaOH solutions were added dropwise until it reached desirable pH values (pH 2, 5, 7 and 8). Turbidity of the samples was determined by measuring absorbance at 500 nm using UV/Vis spectrophotometer after 1 h. The samples for zeta potential analysis of RS, 1 GS, and 96 GS solutions at pH 2, 5, 7, and 8 were also prepared following same procedure of turbidity measurement and the zeta potential was measured using dynamic light scattering (z390, Malvern, UK).

Reversibility of the turbidity and surface charge of the particle depending on the pH was also measured to examine if the pH-induced aggregation is reversible. The 96 GS solutions (pH 2 and 5) were prepared following the same procedure described above. Then, small amount of 1 N NaOH solution was added to the 96 GS solution until it reached pH 7. The turbidity and zeta potential (mV) on each step were measured by UV/Vis spectrophotometer (500 nm) and dynamic light scattering (z390, Malvern, UK), respectively. Then the pH of the solutions was readjusted to pH 2 and 5 to repeat the procedures. The pH adjustment step was done 4 times for the turbidity measurement and 2 times for the zeta potential analysis.

FT-IR analysis on RS, 1 GS, and 96 GS were conducted using an infrared Fourier transform spectrometer (TENSOR27, Bruker, Germany). All samples were measured in a powder form, and the spectral range was 400–4000 cm^{-1} with 32 scans and a resolution was 4 cm^{-1}.

2.4. Loading of curcumin in host solution

The starch-curcumin complexes were prepared by procedure described in Yu and Huang (2010) with minor modification. Host materials (200 mg; MD, CD, 1 GS, and 96 GS) were added in 20 ml of distilled water (1% w/v) and heated at 80 °C to ensure complete dissolution. Then, an excessive amount of curcumin was added to the dispersion with continuous stirring. The mixture was homogenized using a high-speed blender (ULTRA-TURRAX model T25 digital, IKA, Germany) at 12,000 rpm for 10 min and mechanically stirred for 24 h at 60 °C with no light exposure. Undissolved curcumin crystals were removed by centrifugation (9,000 rpm, 15 min) and only the supernatant was collected. The supernatant was frozen at −60 °C overnight and freeze-dried for 4 days for complete dehydration (FD8508, IlShin BioBase, Korea). The final product was grounded into flaky-powders and stored at −20 °C for further analysis. For the stability and bioaccessibility

analysis, complexes were reconstituted by dissolving in distilled water (1% w/v) and heating at 80 °C for 10 min for dissolution. Undissolved solids were removed by centrifugation (12,000 rpm, 10 min) and the supernatant was used for analysis.

2.5. Quantification of curcumin content

In all the experiments, curcumin concentration was measured spectrophotometrically according to Loksuwan (2007) with modification. The complex solution was mixed with 100% DMSO (1:1) to extract curcumin. The mixture was centrifuged (5,000 rpm, 10 min) to remove solids and supernatant was analyzed using UV/Vis spectrophotometer at 430 nm. The curcumin content was calculated based on a curcumin standard curve (50% DMSO; 1–6 μg/mL). All measurements were conducted triplicate.

2.6. Phase solubility

Phase solubility of curcumin with host materials was measured according to the method described by Higuchi and Connors (1965). The host materials (MD, CD, 1 GS, and 96 GS) were dissolved in 2 mL of distilled water (1–6% (w/v)). Excessive amount of curcumin was added to each solution. The suspensions were completely sealed with aluminum foil to prevent photochemical degradation and shaken for 72 h at room temperature until it reached the equilibrium. Aliquots were centrifuged (9,000 rpm, 10 min) to remove solids and only the supernatant was diluted in 100% DMSO (1:1). Curcumin content in the mixtures was assayed spectrophotometrically at 430 nm by using aqueous solutions of the host materials as blanks.

2.7. Characterization of the curcumin complexes

2.7.1. Fourier transform infrared spectroscopy (FT-IR)

In order to determine if there was interaction between curcumin and host materials (MD, CD, 1 GS, and 96 GS), FT-IR spectra analysis was performed using an infrared Fourier transform spectrometer (TENSOR27, Bruker, Germany). The measurements were conducted on curcumin, each host material, physical mixtures, and encapsulated curcumin, and all samples were analyzed in a powder form. The spectral range was 400–4000 cm^{-1} with 32 scans and a resolution was 4 cm^{-1}.

2.7.2. Scanning electron microscopy (SEM)

Morphology of the encapsulated curcumin was observed by Scanning Electron Microscope (SEM) (SUPRA 55VP, Carl Zeiss, Germany). Pure curcumin (Cur), host materials (MD, CD, 1 GS, and 96 GS), physical mixture of curcumin and the host materials, and the encapsulated curcumin were imaged. The samples in a powder form were placed on a carbon tape and coated by Platinum under vacuum condition at 20 mA for 180 s. The thickness of the Platinum coating was 20 nm. The samples were imaged on a scanning electron microscope at an acceleration voltage of 2.00 kV, and micrographs of each sample were taken at 500x, 1000x, and 2000x magnification.

2.8. Stability studies

2.8.1. pH stability

pH stability of curcumin within the complexes was measured according to Ansari and Parveen (2016) with slight modification. Complex solutions (1% w/v) were 2-times diluted with phosphate buffer (10 mM; 1.15 g/L Na_2HPO_4, 0.25 g/L KH_2PO_4; pH 2, 5, 7, 8, and 10). After different time periods (0.5, 1, 2, 3, 5, 7, 24, and 48 h), the solution was centrifuged (9,000 rpm, 10 min) to remove solids. The supernatant was 2-fold diluted and the change in curcumin content was measured spectrophotometrically at 430 nm. Stability of curcumin (Cur), which is a negative control, was also analyzed according to Kharat et al. (2017)

by dissolving stock curcumin in 10% DMSO solution and then diluted with phosphate buffer. Considering possible starch gelation which might affect the turbidity of the curcumin complex solution, we set the turbidity of the starch solution at each pH level as a blank to minimize possible errors. To compare the pH stability of different host materials, the degradation rate constant (k_d) and half-life ($t_{1/2}$) were calculated following simple first-order kinetics (Equations (1) and (2)).

Degradation constant

$$C_t = C_0 e^{-k_d t} \tag{1}$$

where C_t is the curcumin retention at time t (day), C_0 is the initial curcumin content, and k_d is the rate of degradation constants (day^{-1}).

Relationship between k_d and $t^{1/2}$

$$k_d = \ln2/t_{1/2} \tag{2}$$

where $t_{1/2}$ is a half-life constant.

2.8.2. UV stability

Stability of curcumin against UV radiation in the encapsulation system was evaluated by exposing the encapsulated curcumin solution to UV light (TUV 8W G8T5, Philips, Poland). The encapsulated curcumin was reconstituted by dissolving in water. Curcumin dissolved in DMSO solution was also prepared as a negative control. The samples in a clear glass vial were exposed to UV radiation for a set time (0, 1, 2, 4, 6, 8, 10 and 24 h). Then, the sample aliquots were diluted with 100% DMSO solution (1:1) and analyzed spectrophotometrically at 430 nm.

2.9. In vitro simulated digestion

Biological fate of the encapsulated curcumin after digestion was evaluated by *in vitro* simulated digestion assay. The digestion model was referred from the method which has been described in detail in previous studies (Mun, Kim, & McClements, 2015; Sarkar, Goh, & Singh, 2009). Therefore, the method is described only concisely here. The digestion model consisted of three consecutive steps – oral, gastric, and small intestinal phase. Simulated saliva fluid (SSF), simulated gastric fluid (SGF), salt stock, and 10 mM phosphate buffer (pH 7) were prepared as described by Sarkar, Goh, Singh, and Singh (2009). Besides, 15 mL of each reconstituted complex solution was prepared before the oral phase.

2.9.1. Oral phase

Mucin solution was prepared a day before the experiment and stirred overnight, then α-amylase was added to the mucin solution. The mixture was adjusted to pH 6.8 by adding 6 M NaOH solution dropwise. The samples and mucin solution were incubated at 37 °C for 15 min to equilibrate temperature. Afterward, the samples were mixed with the mucin solution at a 1:1 ratio and incubated at 37 °C for 10 min with continuous stirring.

2.9.2. Gastric phase

Pepsin solution was prepared and incubated at 37 °C before the experiment. The pepsin solution was mixed with the sample mixture from the oral phase (1:1) and adjusted to pH 2.5 using 6 M NaOH solution. The sample was incubated at 37 °C for 2 h with continuous stirring using a magnetic bar.

2.9.3. Small intestinal phase

Bile extract and pancreatin was prepared during the stomach step. Samples from the gastric phase was adjusted to pH 7, then bile extract and salt stock were added. The mixture was adjusted to pH 7 again. The pancreatin solution was added and the mixture was incubated at 37 °C for 2 h with continuous stirring. Then, the sample was adjusted to pH 7. Analysis of lipid digestion, which is generally included in the emulsion studies, was omitted here because the encapsulation system in this

study does not contain oil constituent as well as further lipid digestion procedure. Also, the simple GIT model incorporated in this study cannot accurately account for all the events that occur in the human body, as reported in the previous study (Mun et al., 2015).

2.9.4. Curcumin bioaccessibility

Bioaccessibility of curcumin was evaluated after the samples had undergone the simulated digestion system, as described in sec. 2.9.1 - 2.9.3. The final digesta, which went through all the digestion process, was centrifuged (4,000 rpm, 40 min) and the supernatant was collected and assumed to be the "sample" mixture, in which the hydrophobic compound is solubilized. Curcumin in the sample mixture was extracted by adding chloroform at a 1:1 ratio and centrifugation (1750 rpm, 10 min). Only the bottom layer was collected, and the extraction step was repeated 3 times. The chloroform layers were analyzed spectrophotometrically at 430 nm with pure chloroform as a blank. The initial sample before the digestion was set as a control. Concentration of curcumin in the sample mixtures was determined from a curcumin standard curve in chloroform and the bioaccessibility was determined according to the equation (3).

Bioaccessibility = (Curcumin concentration in sample/Initial curcumin concentration) x 100. (3)

2.11. Statistical analysis

All the experiments conducted in this study were performed duplicate or triplicate and expressed as the mean and standard deviation (mean ± SD). For statistical analysis, the one-way ANOVA test followed by Tukey test for mean comparison was processed by IBM SPSS (Version 23.0; SPSS Inc., USA). A *p*-value < 0.05 indicated a statistically significant difference between the data.

3. Results & discussion

3.1. Physicochemical properties of 4αGTase-treated rice starch

3.1.1. Molecular characteristics of 4αGTase-treated rice starch

The Mw distributions of native rice starch (RS), 4αGTase-treated rice starch (1 GS and 96 GS) and MD are presented in Fig. 1a. Native rice starch exhibited two large peaks: an early peak (fraction 1; retention time, 15–30 min) and a later peak (fraction 2; retention time, 32–50 min) as measured by high pressure size exclusion chromatography (HPSEC). The first fraction corresponded to amylopectin and had high Mw, while the second fraction indicated amylose and had low Mw (Do et al., 2012). For 1 GS and 96 GS, both fractions were shifted slightly to the right (fraction 1, 18–31 min; fraction 2, 35–50 min), which is consistent with Takaha, Yanase, Takata, Okada, and Smith (1996). Specifically, the M_p (peak Mw) of the second fraction shifted from 4×10^5 g/mol to 4.73×10^4 g/mol after enzyme treatment. The relative peak intensity of fraction 1 for GS significantly decreased with treatment time, indicating that amylopectin chains were hydrolyzed and molecules with lower Mw formed as a result of enzyme treatment. On the other hand, the relative intensity of the second fraction significantly increased with enzyme treatment, resulting in 2.52-fold higher peak intensity for 96 GS than 1 GS. The increased peak intensity of the second fraction was attributed to degradation and disproportionation of amylopectin and amylose, which reorganized modified amylopectin clusters by 4αGTase activity (Oh, Choi, Lee, Kim, & Moon, 2008). Enzymatic treatment resulted in an overall decrease in the average Mw of GS compared to RS. In addition, the average Mw of the MD (DE 8–10) was lower than the 96 GS ($M_p \approx 4.73 \times 10^4$ g/mol) with M_p at a retention time of 50 min.

Branched chain length distributions of MD, RS, 1 GS, and 96 GS after isoamylase treatment were measured by high-performance anion
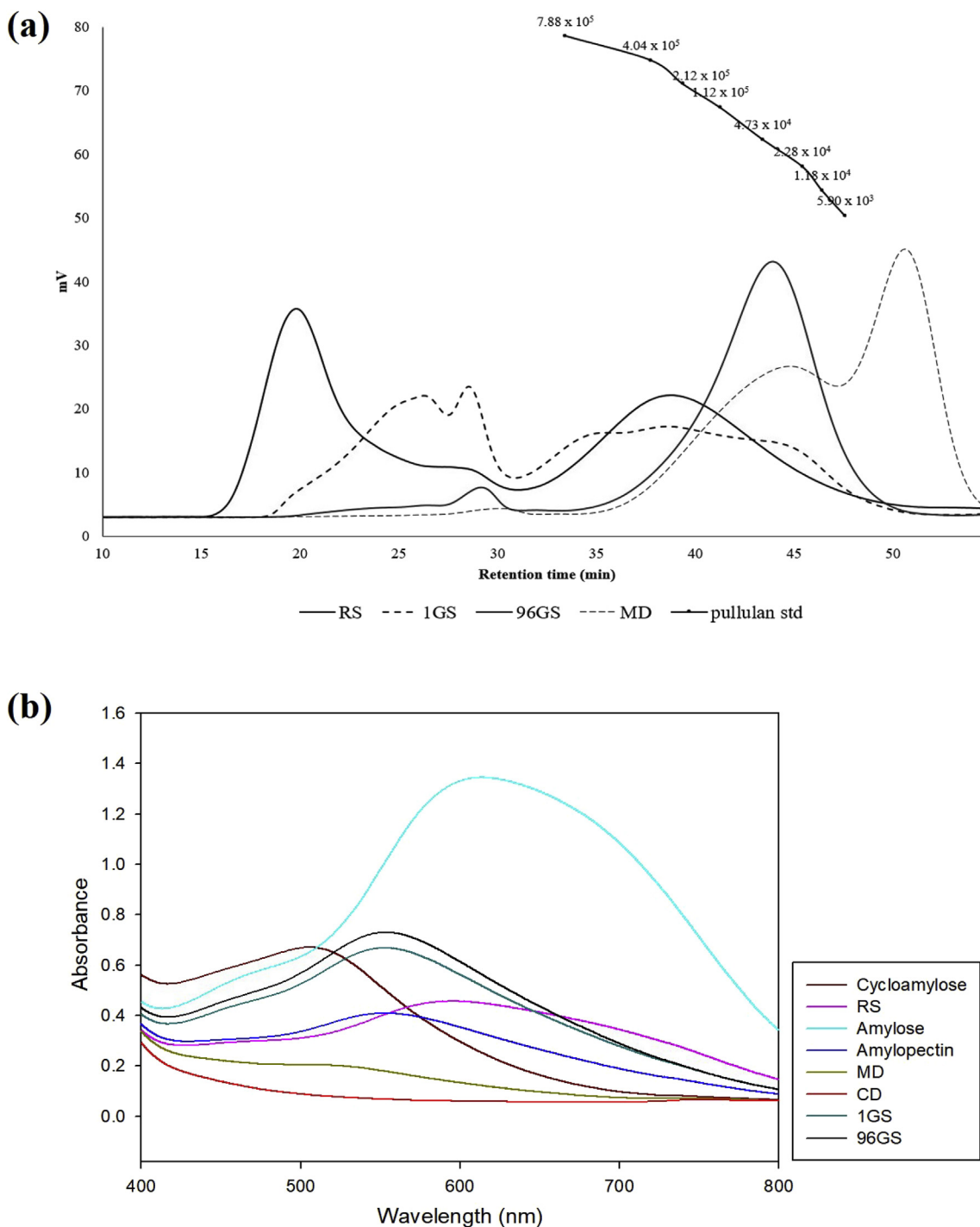
Fig. 1. (a) Molecular weight distribution of maltodextrin (MD), native rice starch (RS), and 4αGTase-treated rice starch (1 GS and 96 GS) with pullulan standard, (b) Wavelength scanning profile of host materials (RS, MD, β-cyclodextrin (CD), 1 GS, 96 GS, cycloamylose, amylose, amylopectin) binding iodine.

Table 1
Rate of branched chain length (%) of MD, RS, 1 GS and 96 GS.

Host material	Chain length distribution (%)			
	A	B₁	B₂	B₃
	DP ≤ 12	DP 13-24	DP 25-36	DP > 36
MD	77.24	20.26	2.50	-
RS	32.04	50.55	12.35	5.05
1 GS	34.69	40.95	17.42	6.93
96 GS	38.00	38.25	16.82	6.93

exchange chromatography (HPAEC) (Table 1). MD exhibited a chain length distribution with degree of polymerization (DP) ranging from 2 to 32. The highest proportion of chains had a DP of 3–4, and the proportion gradually decreased with increasing DP. The chain length distribution of RS had a mountain-like shape, with a peak at DP 10 and a tail-like section from DP 30 to 60 (Data not shown). However, 1 GS and 96 GS had much broader and flatter distributions from DP 2 to DP 62. RS had a lower proportion of A chains and B₃ chains (A, 32.04%; B₃, 5.05%) than MD (A: 77.24%) and GS (A, 34.69–38%; B₃, 6.93%). RS also had a higher proportion of B₁ and B₂ chains, which is consistent with previous studies (Do et al., 2012; Kim et al., 2012; Park et al.,
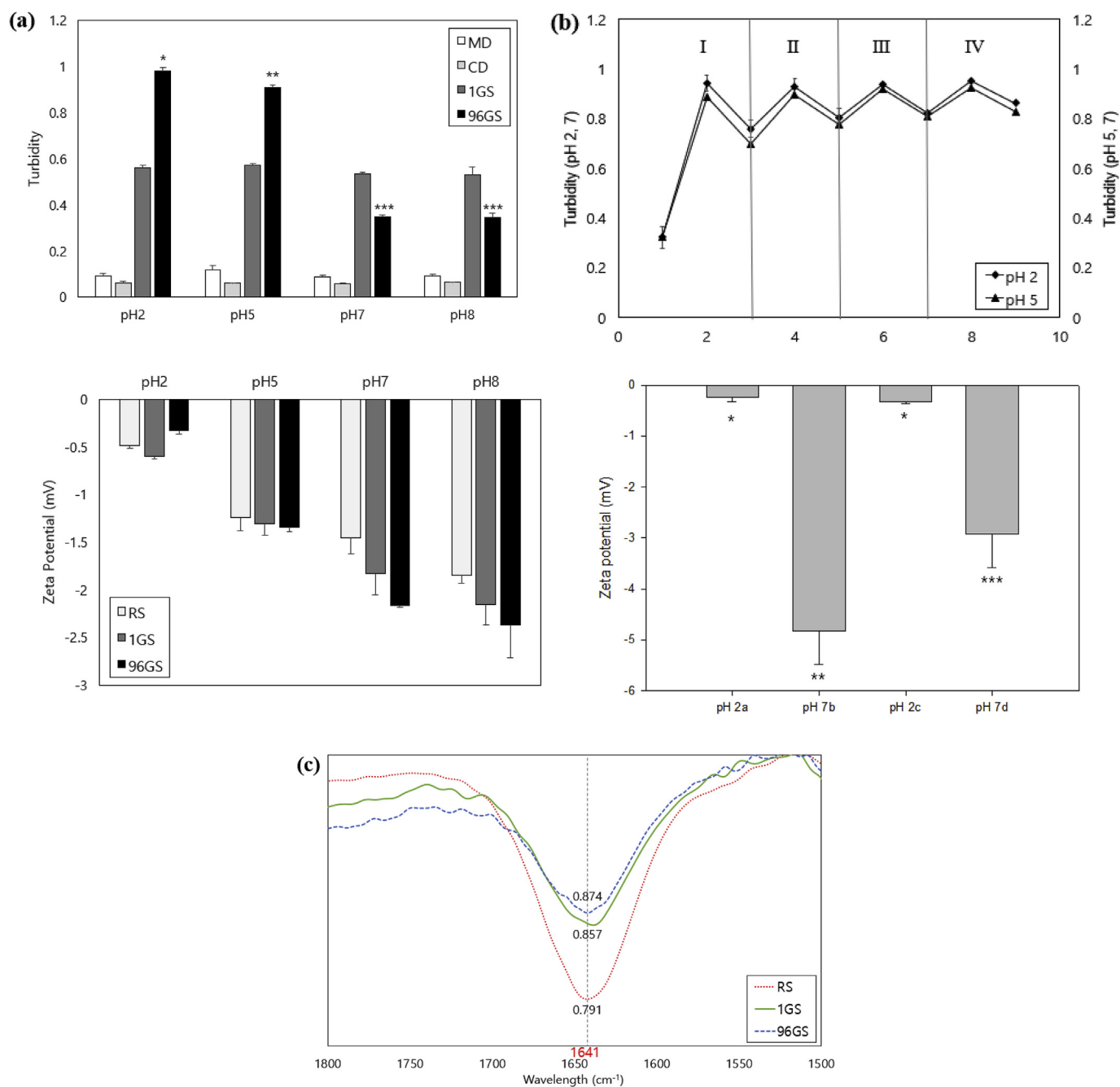
Fig. 2. (a) Turbidity of MD, 1 GS, and 96 GS solution (5% w/v) at pH 2, 5, 7, and 8 (top) and zeta potential of RS, 1 GS, and 96 GS solution at pH 2, 5, 7, and 8 (bottom); (b) turbidity reversibility of the 96 GS solution at pH 2 and 5 (top) and zeta potential reversibility of 96 GS solution at pH 2 and 7 (bottom); (c) FT-IR spectra of RS, 1 GS, and 96 GS in between wavelength of 1,500–1,800 cm^{-1}.

2007). The relative area of the B_1 chain (DP 13–24) decreased after 4αGTase treatment, whereas the relative area of A (DP ≤ 12) increased (1 GS, 34.69%; 96 GS, 38%). In particular, the large peak at DP 3 observed for 96 GS indicates that 4αGTase treatment increased the proportion of very short amylopectin glucan chains. This may be because the external chains of amylopectin are more susceptible to the disproportionation reaction, resulting in the short external chains being more disproportionated and redistributed through the treatment (Do et al., 2012). The relative proportion of the long chains (B_2 and B_3; DP > 25) decreased slightly with increasing treatment duration (1 GS, 24.35%; 96 GS, 23.75%). Changes in the chain length distribution after 4αGTase treatment might be due to intermolecular disproportioning activity by 4αGTase, which transfers α-glucan chains from one to

another. Previous studies suggested that the inner chains of amylopectin clusters (specifically, the B and C chains) were cleaved in addition to outer chain trimming, resulting in a change in the length of branched chains (Cho Auh, Kim et al., 2009; Cho Auh, Ryu et al., 2009; Do et al., 2012; Kaper, Maarel, Euverink, & Dijkhuizen, 2004). Transfer of α-glucan chains occurred in both the amylose and amylopectin fractions, as described by Kaper et al. (2004). Moreover, 4αGTase activity is known to result in the formation of cyclic glucans with various DPs. Cho Auh, Kim et al., (2009); Cho Auh, Ryu et al., (2009) argued that the matrix-assisted laser desorption/ionization time of flight mass spectrometry (MALDI-TOF-MS) signals corresponding to cyclic glucans with DP 5–19 strongly increased after 4αGTase treatment of rice starch. Park et al. (2007) also suggested that the DP of cyclic glucans produced

from 4αGTase treatment ranged from about 19 to 35, based on HPAEC and MALDI-TOF data. Therefore, the increased proportion of short and middle chains (DP 5–35) in GS may be attributed partly to the formation of cyclic glucans after 4αGTase treatment.

3.1.2. Complex formation capacity

The complex formation capacity of the MD, CD, RS, 1 GS and 96 GS was evaluated by iodine absorption measurements (Fig. 1b). MD and CD showed relatively flat spectra with no observable peaks. The complex formed between the amylose standard and iodine had a deep blue color, with the highest absorbance occurring at a peak wavelength of 612 nm). RS solution also turned light blue when complexed, indicating that iodine was bound mainly to the linear helixes of amylose. Meanwhile, a light purple color appeared in the amylopectin-iodine complex, which is consistent with a previous study suggesting that amylopectin has a lower capacity to form iodine complexes than amylose (Bailey & Whelan, 1961). Different complexation properties between amylose and amylopectin may result from differences in chain length distribution and branching structure (Shen, Bertoft, Zhang, & Hamaker, 2013). The peak wavelength of RS ($\lambda_{max} \approx 592$ nm) was in the middle of the peak wavelength of amylose and amylopectin ($\lambda_{max} \approx 557$ nm), possibly because both components were involved in iodine complexation.

Kearsley and Dziedzic (1995) also reported that both amylose and amylopectin in starch could bind iodine and develop specific colors according to the DP of chains (DP > 47, blue; DP39–46, blue-violet; DP30–38, red-violet; DP25–29, red; DP < 20, no color). In other words, maximum absorbance (λ_{max}), which is also an index of iodine complexation, is proportional to the DP of starch up to a DP of about 100 (Bailey & Whelan, 1961). In the case of GS, both 1 GS and 96 GS had a deep violet color with a leftward shift of the wavelength ($\lambda_{max} \approx 554$ nm). This may be attributed to an increase in the number of molecules with DP 30–48 as a result of enzyme treatment. The peak wavelength of the 4αGTase-treated starches was close to the peak wavelength of amylopectin, suggesting that the complex formation capacity of the enzyme-treated starches may depend on amylopectin content. Moreover, 96 GS exhibited higher absorbance than 1 GS (1 GS, 0.669; 96 GS, 0.73) and λ_{max} similar to the cycloamylose standard (0.67; $\lambda_{max} \approx 509$ nm). The maximum peak wavelength for GS was intermediate between the wavelengths of cycloamylose and RS, indicating that both cyclic glucans may have acted as complexing agents with iodine. Given that 4aGTase treatment of amylose causes (a) the transfer of amylose chains to amylopectin branch chains by intermolecular transglycosylation and (b) the formation of cyclic glucans by intramolecular transglycosylation (Do et al., 2012), the increased complex-forming ability of 96 GS may be attributable to the increased number of longer side chains with DP ≧ 34 and the formation of cyclic glucans.

3.1.3. pH-induced aggregation of 4αGTase-treated rice starch

During the pH stability analysis of the encapsulated curcumin, we observed that the turbidity of 96 GS changed depending on environmental pH. Hence, we measured the turbidity of MD, CD, RS, 1 GS, and 96 GS at pH 2, 5, 7, and 8. Turbidity of RS was significantly higher than other host materials at any pH condition because of gelation contributed by large molecular weight and chain length distribution (data not shown). As shown in Fig. 2a (top), MD, CD and 1 GS did not significantly differ in turbidity among pH conditions. However, the turbidity of 96 GS solution at pH 2 (0.98 ± 0.02) was almost 2.8-fold higher than at pH 8 (0.35 ± 0.02) ($p < 0.05$).

In addition, the pH-dependent increase in the turbidity of the 96 GS solution was partially reversible (Fig. 2b [top]). After the first pH readjustment from 2 to 7, the turbidity of the 96 GS solution decreased from 0.94 (pH 2a) to 0.76 (pH 7a). When the pH of the solution returned to 2b, turbidity increased to 0.93 from 0.76. It also decreased to 0.80 (pH 7b) and increased to 0.93 (pH 2c) with subsequent pH adjustments. During the first four cycles, turbidity repeatedly increased

and decreased depending on pH, although the magnitude of these changes gradually decreased. Similar results were found for the zeta potential measurement. To confirm whether the aggregation was related to surface charge of starch particles, we also measured zeta potential of the 96 GS at pH 2 and 7. As shown in Fig. 2b (bottom), zeta potential of the 96 GS solution significantly changed depending on pH. The absolute zeta potential of the 96 GS solution at pH 2 was 0.246 mV, but it sharply increased to 4.82 mV as pH increased to 7. It again decreased to 0.319 mV with decreased pH, then increased to 2.91 mV as the pH was readjusted to 7. In addition, zeta potential of the RS, 1 GS, and 96 GS solution at pH 2, 5, 7, and 8 were also evaluated. As a result, all of them were found to be negatively charged at all pH as well as the charge was lowest under acidic condition (Fig. 2a [bottom]). The 96 GS showed the greatest differences in charge by the pH conditions, which corresponded to the turbidity results, and it suggests that it was most affected by pH conditions. Unlike 96 GS, change in the zeta potential of RS and 1 GS solution would not have had much effect on the turbidity of the solution as they quickly formed turbid gels by themselves owing to large molecular weight, irreversible gelation and their turbidity formed by self-networking. Moreover, degree of enzyme treatment of the 1 GS is relatively lower than that of 96 GS so that its functionality is more like RS than the 96 GS.

A previous study argued that aggregation or flocculation of starch was mainly due to the van der Waals effect and hydrogen bonding, although surface charge would be expected to repulse particles from one another (Liu, Wu, Chen, & Chang, 2009). Given that the turbidity results of 96 GS corresponded to the zeta potential results in the present study, the change in the turbidity by pH may be attributed to the change in the surface charge of the 96 GS. In short, decreased repulsion forces may have promoted H-bonding and aggregation. Furthermore, FT-IR spectra of RS, 1 GS, and 96 GS were analyzed to confirm how the molecular aspects have been altered after the enzyme treatment. According to Fig. 2c, strong peaks from 1,500 cm^{-1} to 1,750 cm^{-1}, which correspond to the carbonyl group (C=O) appeared with different peak intensities by the degree of enzyme treatment. In particular, the C=O peak intensity of the RS (0.791) was lower than those of 1 GS (0.857) and 96 GS (0.874). Also, the 96 GS peak intensity was higher than that of 1 GS, which suggests that the enzyme treatment might have increased density of carbonyl groups of starch molecules. Therefore, based on these results, it was suspected that the main factor that promoted aggregation of the 96 GS under acidic condition might be possible oxidation occurred during the enzyme treatment process. In other words, the oxidation might have oxidized -OH of the starch molecule into the carbonyl group, resulting in negatively charged polymers in solution. Based on this interesting finding, further research on detailed identification of the underlying mechanisms of the pH-dependent behavior of 96 GS and its application such as pH-triggered aggregation is anticipated.

3.2. Encapsulation of curcumin

3.2.1. Phase solubility

Phase solubility measurements of curcumin with MD, CD, 1 GS, and 96 GS (0–6%) were carried out at room temperature (Fig. 3a). At 6% (w/v) concentration, MD, 1 GS and 96 GS improved curcumin solubility by approximately 2,497-, 2,241- and 2,846-fold, respectively, compared to pure curcumin (Cur; appx. 11 ng/mL; Kaminaga et al., 2003). The phase solubility of curcumin with 96 GS gradually increased with increasing 96 GS concentration, while the solubility plots of curcumin with 1 GS showed a gradual increase up to 5% (w/v) and a plateau at higher concentrations. These results are largely consistent with a previous study, which suggested 18.4 μg/mL of curcumin was solubilized when 1% HMS solution was incorporated during curcumin encapsulation (Yu & Huang, 2010), The solubility of curcumin encapsulated by host materials was significantly different from Cur ($p < 0.05$), and did not differ depending on the type of host material. According to Higuchi
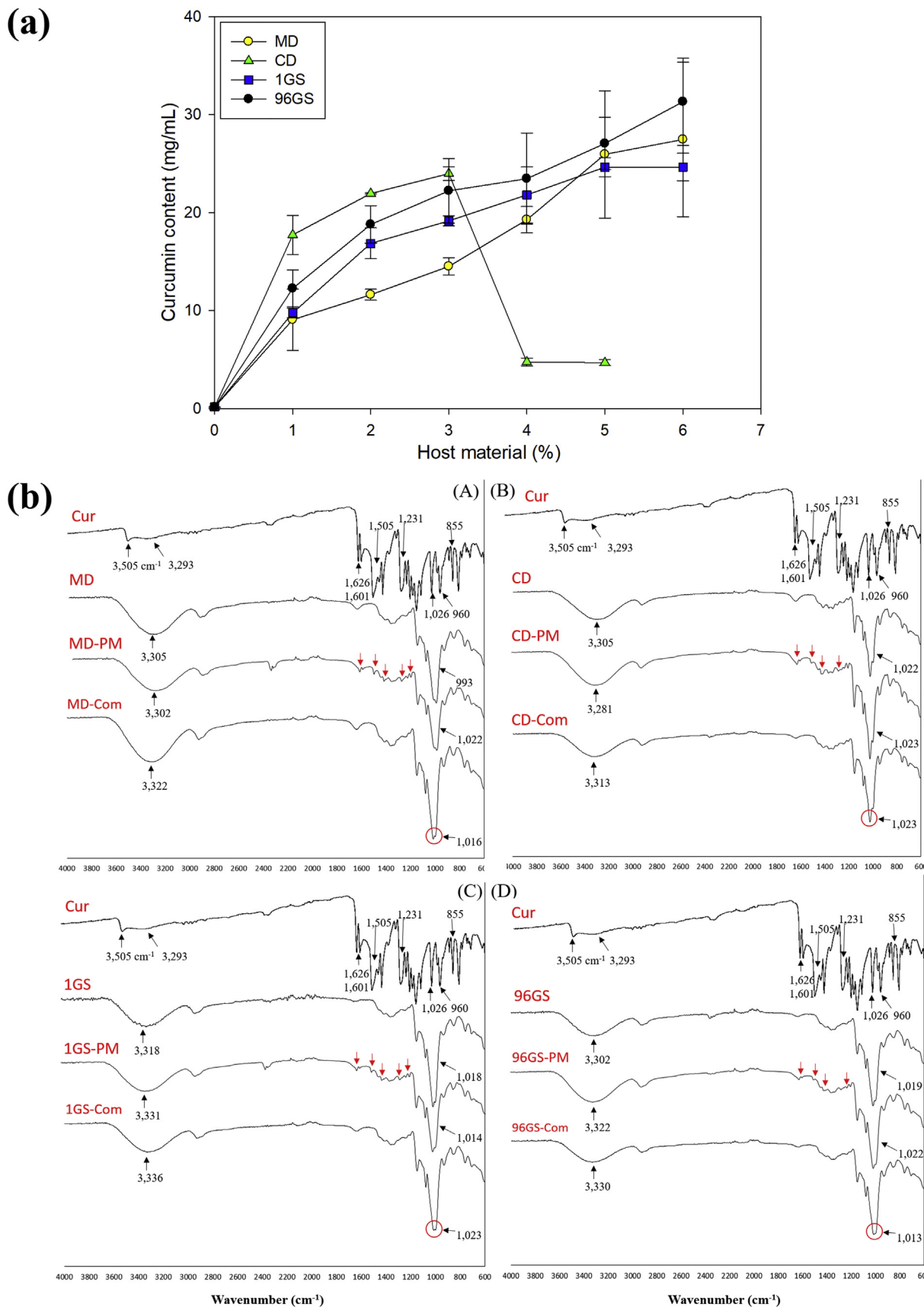
Fig. 3. (a) Phase solubility diagram of curcumin encapsulated with MD, CD, 1 GS, and 96 GS. (b) FT-IR spectra of Cur, host materials ((A) MD, (B) CD, (C) 1 GS, and (D) 96 GS), physical mixtures (-PM), and complexes (-Com).

and Connors (1965), phase solubility diagrams of drug materials can be classified into type A or B according to their ability to form soluble inclusion complexes. A-type curves suggest the formation of soluble complexes, while B-type curves indicate the formation of complexes with low water solubility. A-type curves can be further divided into A_L, A_P and A_N according to their dissolution patterns. Based on this framework, the solubility diagram of curcumin with 96 GS can be classified as the A_L type, reflecting a linear increase in curcumin solubility as a function of the concentration of the host material. On the other hand, 1 GS gave rise to an A_N-type curve owing to the limited solubility of the starch itself. This result is consistent with the observation of Jain, Date, Pissurlenkar, Coutinho, and Nagarsenker (2011) that the A_L-type curve may be observed with highly water-soluble compounds. The main differences between the 1 GS and 96 GS solubility curves may be attributed to average Mw. According to Brazel and Rosen (2013), the solubility of polymers depends on their physical and chemical properties, such as polarity, Mw, branching and degree of crosslinking. In particular, the authors claimed that the solubility of polymers decreases with increasing Mw at a particular temperature. Furthermore, a previous study suggested that soluble carbohydrates from sorghum couscous consisted of low Mw molecules as well as a large portion of branched starch molecules (Aboubacar & Hamaker, 2000). Moreover, 96 GS may contain a greater amount of cycloamylose, which is known to form inclusion complexes with hydrophobic properties, compared to 1 GS as a result of 4αGTase treatment. A previous study argued that the complexation of a rarely soluble compound with cycloamylose significantly increased the solubility of the hydrophobic compound (Tomono et al., 2002). Therefore, the narrower chain length distribution, lower average Mw and higher amount of cycloamylose for 96 GS may have increased its solubility.

The phase solubility of curcumin with MD was lower than both 1 GS and 96 GS up to the concentration of host materials of 4%, while the difference became insignificant among samples at the concentration higher than 5%. The lower phase solubility of curcumin with MD than GS may be attributed to their different structural properties. Unlike MD, GS consists of cycloamylose and amylopectin clusters with elongated side chains (Kaper et al., 2004), which could have improved curcumin phase solubility not only by physical encapsulation but also by complexation, as also discussed above. In other words, different molecular composition and structural properties of MD and GS might result in higher phase solubility of curcumin with GS than MD.

The phase solubility of curcumin with CD followed a different trend compared to GS and MD. Solubility gradually increased up to 3% (w/v) of CD with a noticeable decrease at concentrations higher than 3% (w/v). Also, CD resulted in a 2,180-fold increase in the solubility of curcumin; maximum curcumin solubility was 23.99 μg/mL at a CD concentration of 3% (w/v). The solubility diagram of CD-curcumin can be classified as a B-type curve, specifically B_S, as suggested by Higuchi and Connors (1965). The decrease of phase solubility at high CD concentrations can be explained by its low water solubility. Previous studies reported that the solubility of CD is about 1.85% (w/v) in pure water, which is relatively low compared to other starch derivatives (Miranda, Martins, Veiga, & Ferraz, 2011). Considering the low water solubility of CD itself and the sharp decrease in phase solubility at high CD concentrations, it is possible that undissolved CD after saturation may have interrupted the complexation between CD and curcumin, resulting in lower solubility. However, the maximum amount of curcumin solubilized with CD did not differ significantly from that with MD, 1 GS, and 96 GS ($p > 0.05$). Additionally, we suggest that the use of CD in curcumin encapsulation systems may be limited to small-scale production, since curcumin solubility decreases at concentrations above 3% (w/v). Conversely, MD, 1 GS and 96 GS are more suitable for mass-production systems that incorporate high concentrations of host materials.

3.2.2. Characterization of the curcumin complexes

3.2.2.1. Fourier transform infrared spectroscopy (FT-IR). The FT-IR peak assignments were analyzed to assess potential interactions between curcumin and host materials. The FT-IR spectra of Cur, host materials (MD, CD, 1 GS, and 96 GS), the physical mixture of curcumin with each host material (-PM), and encapsulated curcumin within the host materials (-Com) are shown in Fig. 3b. Within the curcumin spectrum, there was a small and sharp peak at $3,505\,cm^{-1}$ and a broad and weak peak at $3,293\,cm^{-1}$, indicating the presence of -OH. The strong peaks at $1,626\,cm^{-1}$ and $1,601\,cm^{-1}$ corresponded to C=C and C=O conjugation, respectively. In particular, the peak at $1,601\,cm^{-1}$ was associated with stretching of the benzene ring of curcumin (Li, Shin, Lee, Chen, & Park, 2016). The peaks at $1,505\,cm^{-1}$ and $1,274\,cm^{-1}$ were attributed to C=O vibration and enol C-O, respectively. The sharp absorption bands at $1,026\,cm^{-1}$ and $855\,cm^{-1}$ represented C-O-C stretching, and the peak at $960\,cm^{-1}$ was determined to be benzoate trans -CH (Mohan et al., 2012). The peak at $1,231\,cm^{-1}$ was assumed to be aromatic C-O stretching vibrations.

The spectra of physical mixtures were essentially combinations of the peaks from Cur and host materials. In other words, all the major sharp peaks belonging to Cur were observed in the spectra of the physical mixtures. Specifically, the major peaks of curcumin ($1,626\,cm^{-1}$, $1,601\,cm^{-1}$, $1,505\,cm^{-1}$, $1,427\,cm^{-1}$, $1,231\,cm^{-1}$, $1,203\,cm^{-1}$, $1,026\,cm^{-1}$, $1,022\,cm^{-1}$, $960\,cm^{-1}$, and $855\,cm^{-1}$) appeared on the PM spectra, even though there was a difference in peak intensity depending on the type of host material.

On the other hand, all of the FT-IR spectra of the encapsulated curcumin within the host materials were almost identical to the spectra of the host materials. In the spectra of MD-Com, the peak for -OH stretching vibration and C-O-C stretching of MD was shifted from $3,305\,cm^{-1}$ to $3,322\,cm^{-1}$, and from $993\,cm^{-1}$ to $1,016\,cm^{-1}$, after encapsulation. CD-Com also showed two band shifts from $3,305\,cm^{-1}$ to $3,313\,cm^{-1}$ and from $1,022\,cm^{-1}$ to $1,023\,cm^{-1}$. In the 1 GS-Com spectra, the -OH stretching peak was shifted after encapsulation, from $3,318\,cm^{-1}$ to $3,336\,cm^{-1}$. There was also a band shift in the C-O-C stretching vibration ($1,018\,cm^{-1}$ to $1,023\,cm^{-1}$). Likewise, the 96 GS-Com spectra showed a change in the major peaks ($3,302\,cm^{-1}$ to $3,330\,cm^{-1}$ and $1,019\,cm^{-1}$ to $1,013\,cm^{-1}$). This may be because the fingerprint peaks of the curcumin spectra disappeared as the curcumin interacted with the host materials. Apart from the disappearance of the curcumin peaks on the complex spectra, the band shifts can also be considered as an indicator of the interaction between core and host materials (Mohan et al., 2012). The complex fingerprint signals of all types of complexes moved to higher or lower wavelengths, as described above. From these results, it is possible that all host materials may have interacted with curcumin in the complexes.

Previous studies have reported that band shifts occurring in the spectra after encapsulation are most likely due to interactions between starch and curcumin (Li et al., 2016; Mangolim et al., 2014; Rachmawati et al., 2013; Yu & Huang, 2010). In particular, the interactions occur mainly at the -OH and C-O stretching vibrations of the starch and curcumin, as indicated by the fingerprint band shifts on the spectra (Fig. 3b). Li et al. (2016) encapsulated curcumin using soluble starch and claimed that -OH groups of curcumin and glucose units formed hydrogen bonds. Similar, Yu and Huang (2010) identified the formation of hydrogen bonds between starch and curcumin when the curcumin was encapsulated using HMS. Therefore, the major interactions that occurred in the present study between the host materials, including the GS and curcumin, may be attributed mainly to hydrogen bonding.

3.2.2.2. Scanning electron microscopy (SEM). Based on the possible interactions between curcumin and host materials indicated by the infrared spectrum (sec. 3.2.2.1), the morphology of Cur, host materials (MD, CD, 1 GS, and 96 GS), physical mixtures of the hosts and curcumin
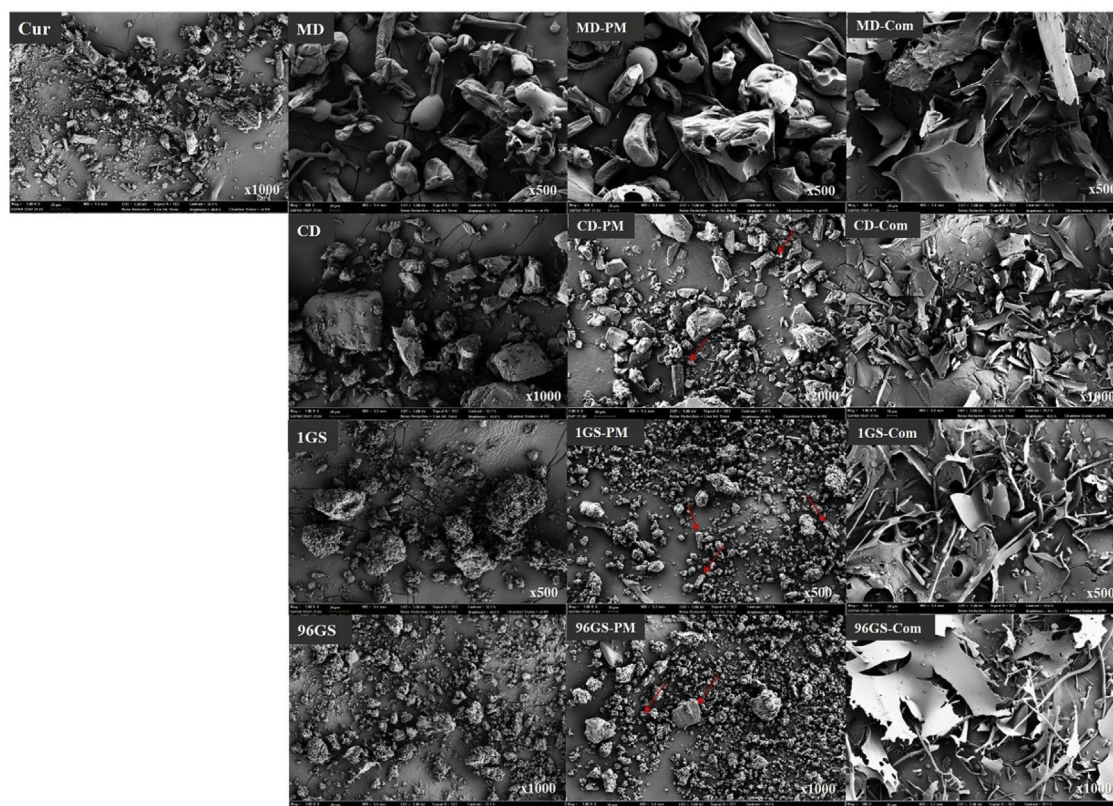
Fig. 4. Scanning electron microscopy: Cur (x1,000), MD (x500), CD (x1,000), 1 GS (x500), 96 GS (x1,000); Physical mixtures (-PM, x 500–2,000); Complexes (-Com, x 500–1,000).

(PM), and complexes were observed via SEM (Fig. 4a). MD and CD had very irregularly shaped particles of various sizes, while 1 GS and 96 GS had masses of tiny particles. The average particle size of GS was much smaller than MD and CD, possibly because they underwent ethanol-promoted precipitation. Curcumin appeared as rod-like long particles, and the particle size was similar to that of the GS. Physical mixtures of the curcumin and each host material appeared as a combination of intact curcumin and parent host material compounds. With respect to complexes, CD-Com had an angular and pointed shape, while the rest (MD, 1 GS, and 96 GS) had much larger flake-like shapes. The latter complexes also formed a glossy surface, implying the formation of amorphous glasses as also indicated by our X-ray diffractometry measurements on the freeze-dried GS (Data not shown). The flake-like shapes of MD, 1 GS, and 96 GS-Com might be attributed to the freeze-drying process during encapsulation. Moreover, Kaushik and Roos (2007) encapsulated limonene by freeze-drying using gum Arabic-sucrose-gelatin systems and proposed that the formation of amorphous glasses during dehydration protected the entrapped molecules from exposure to heat and oxygen. Therefore, the structure of the freeze-dried complexes may have contributed to curcumin protection.

3.2.3. Stability studies

3.2.3.1. pH stability. The low pH stability of curcumin is a significant drawback in food system applications. As previously discussed, curcumin undergoes rapid degradation under alkaline pH conditions and is crystallized under acidic pH. Therefore, we examined the degree to which the encapsulation system could increase curcumin stability under various pH conditions. pH stability was evaluated by suspending curcumin complexes in phosphate buffer adjusted to pH 2, 5, 7, 8 and 10 and measuring the retention (%) of curcumin at regular time intervals. The degradation rate constant (k_d, 10^{-2}/day) and half-life ($t_{1/2}$, day) were calculated based on the curcumin retention after 24 h (Table 2). Cur was about 2.5-fold more likely to be degraded at pH 10

($k_d \approx 1.920 \pm 0.058$) than pH 2 ($k_d \approx 0.771 \pm 0.058$), and the stability of curcumin differed significantly under acidic, neutral and alkaline pH ($p < 0.05$). This result is consistent with previous studies showing that curcumin is more stable under acidic conditions (Kharat et al., 2017).

The encapsulated curcumin was more stable under acidic conditions (pH 2 and 5) than under neutral or alkaline pH conditions, regardless of the type of host material. The curcumin encapsulated with 96 GS had the highest degradation rate ($k_d \approx 0.646 \pm 0.082$) (at pH 2, $p < 0.05$; at pH 5, $p > 0.05$). The curcumin encapsulated within 1 GS was most stable at acidic pH. 1 GS did not differ significantly from host materials but was significantly different from the control ($p < 0.05$). The low stability of the 96 GS-encapsulated curcumin may be attributed to its unique physicochemical characteristics. Aggregated starch of a vivid yellow color was observed in 96 GS samples at acidic pH (pH 2 and 5), while such large aggregations were not observed in 1 GS samples (Data shown in supplementary data). In other words, the aggregation occurred only in the 96 GS samples and only under acidic conditions. This may be attributed to the pH-induced aggregation of 96 GS, as suggested in sec. 3.1.3. The curcumin crystals formed under low pH might have coalesced together as the 96 GS mingled at acidic pH, resulting in low curcumin retention.

96 GS was markedly superior at neutral and alkaline pH values (pH 7, 8, and 10), exhibiting a lower degradation rate than CD or Cur. MD had the lowest degradation rate constant at pH 8, although there was no significant difference between MD and GS ($p > 0.05$). Meanwhile, the difference between CD and GS was statistically significant at pH 8 and 10, indicating that GS had better shielding effects than CD under alkaline conditions. In addition, an initial change in the color of the encapsulated curcumin solutions (from yellow to orange or red) was observed. This may have been because curcumin underwent hydrolytic degradation, so that its condensation products affected color, as described by Kharat et al. (2017). In particular, the curcumin

Table 2
Effect of pH condition on curcumin stability in capsules with host materials after storage in the phosphate buffer.

Host material	pH stability (k_d, 10^{-2}/day)				
	pH 2	pH 5	pH 7	pH 8	pH 10
MD	0.211 ± 0.065^a	0.199 ± 0.038^a	0.252 ± 0.027^a	0.326 ± 0.047^a	$0.465 \pm 0.034^{a,b}$
CD	0.169 ± 0.046^a	0.191 ± 0.033^a	0.342 ± 0.059^a	0.653 ± 0.060^b	0.595 ± 0.120^b
1 GS	0.115 ± 0.022^a	0.089 ± 0.023^a	0.217 ± 0.030^a	0.387 ± 0.043^a	0.349 ± 0.019^a
96 GS	0.646 ± 0.082^b	0.286 ± 0.227^a	0.237 ± 0.057^a	0.340 ± 0.087^a	0.359 ± 0.085^a
Cur	0.771 ± 0.058^b	0.731 ± 0.020^b	1.008 ± 0.050^b	1.743 ± 0.017^c	1.920 ± 0.097^c

Host material	pH stability ($t_{1/2}$, day)				
	pH 2	pH 5	pH 7	pH 8	pH 10
MD	$3.551 \pm 0.493^{a,b}$	$3.549 \pm 0.633^{a,b}$	2.278 ± 0.288^a	2.161 ± 0.337^c	$1.496 \pm 0.106^{b,c}$
CD	4.346 ± 0.576^b	$3.694 \pm 0.614^{a,b}$	2.072 ± 0.399^a	$1.067 \pm 0.094^{a,b}$	1.199 ± 0.254^b
1 GS	6.187 ± 1.707^b	8.058 ± 1.795^c	3.227 ± 0.422^a	1.805 ± 0.193^c	1.988 ± 0.108^c
96 GS	1.084 ± 1.641^a	$3.396 \pm 1.847^{a,b}$	3.027 ± 0.643^a	2.121 ± 0.476^c	1.997 ± 0.415^c
Cur	0.902 ± 0.066^a	0.949 ± 0.027^a	0.689 ± 0.034^b	0.398 ± 0.003^a	0.362 ± 0.019^a

encapsulated with CD exhibited the most rapid and persistent color change (Data not shown). The CD-encapsulated curcumin also had a significantly higher degradation rate constant under alkaline pH (8 and 10), as presented in the results. The low pH stability of the CD-encapsulated curcumin may be attributable to the curcumin being more likely to be exposed to the solvent when encapsulated with CD compared to MD and GS. The relatively weak shielding effect of CD is consistent with a previous study, which reported that the presence of CD only slightly affected curcumin stability, specifically under strongly alkaline conditions (Mangolim et al., 2014). In fact, CD is known to form a complex with curcumin through the entry of an aromatic ring of curcumin into the cavity, so that some proportion of the curcumin may have been exposed to the environment, promoting rapid degradation. Moreover, CD had the lowest Mw (1,135 g/mol; Del Valle, 2004) among the host materials, which may have been insufficient to provide shielding effects beyond those of complexation.

The 1 GS-encapsulated curcumin exhibited the highest stability under all pH values except pH 8, at which MD- and 96 GS-encapsulated curcumin were marginally more stable ($p > 0.05$). The increased pH stability provided by GS and MD can be attributed to their shielding effects from hydrolytic interactions (Tonnesen et al., 2002). According to Li et al. (2016), the formation of hydrogen bonds between curcumin and starch may prevent curcumin hydrolysis triggered by the environment. Therefore, the more interactions that occur between curcumin and polymer, the greater the degree of protection of curcumin. Moreover, as sec. 3.1.1. suggested, 1 GS and 96 GS have more branched chains than MD and CD, which should increase the likelihood of interactions with bioactive compounds. These results suggest that 1 GS is capable of protecting curcumin under all pH conditions, and that 96 GS also works within a limited pH range (pH 7 and above).

3.2.3.2. UV stability. Curcumin is known to be degraded very quickly under UV radiation, which it may be exposed to during the sterilization or distribution process (Lee et al., 2013; Mangolim et al., 2014). Therefore, a protection system is required to minimize the degradation of curcumin (Paramera et al., 2011). In the present study, we evaluated the UV stability of Cur, and of curcumin encapsulated using MD, CD, 1 GS and 96 GS, after exposure to UVC. We measured the retention (%) of curcumin at various time points over a 24 h period. We compared the UV stability of the encapsulated curcumin to that of Cur (control) dissolved in dimethyl sulfoxide (DMSO) solution. As shown in Fig. 5a, the retention of Cur sharply decreased upon UVC exposure, although it was higher than that of encapsulated samples within the first 8 h. The retention decreased rapidly after 8 h and was 28% after 24 h. The higher initial curcumin retention of the control may be attributed to the type of solvent used to dissolve the solid curcumin. The control curcumin was dissolved in

DMSO owing to its low solubility in water (11 ng/mL water). Mondal, Ghosh, and Moulik (2016) evaluated the rate of curcumin degradation in different media at 303 K and found that curcumin in water had a 156-fold higher degradation rate than curcumin in DMSO. Lee et al. (2013) found that the residual curcumin level (%) was only about 40% after UV radiation for 8 h, while in the present study it was 66%. Therefore, we consider the higher initial retention rate of Cur to be due to the effects of the solvent used.

The retention of encapsulated curcumin tended to decrease sharply within the initial 8 h of exposure, and to decrease at a lower rate after 8 h compared to the control. In particular, about 59.5% of curcumin remained after 24 h exposure, when it was encapsulated with 96 GS, which was about 2.1-fold higher than the control ($p < 0.05$). The CD-cur and MD-cur complexes resulted in lower mean curcumin retention (MD, 39.2%; CD, 41.5%), which is consistent with previous findings regarding the low photochemical stability of curcumin complexed with CD (Paramera et al., 2011; Tonnesen et al., 2002). Previous studies found that the formation of inter- and intra-molecular bonds may have caused destabilizing effects and were not suitable for curcumin protection against UV radiation. The 1 GS-cur also increased the mean retention of curcumin (45.1%), but there was no significant difference from the control (28.6%) ($p > 0.05$).

One factor that may have influenced the UV stability of encapsulated curcumin is the occurrence of hydrogen bonding between the curcumin and host materials (i.e., the 'complexation effect'). Li et al. (2016) argued that hydrogen bonding with starch may have protected curcumin from photochemical degradation. They also reported that curcumin lost two hydrogen atoms per molecule when it underwent photochemical degradation, regardless of its state (Mangolim et al., 2014). Thus, we assumed that the formation of hydrogen bonds between –OH of curcumin and –OH or C-O-C of starch, as suggested by the FTIR spectra (sec. 3.2.2.1), may have hindered the loss of hydrogen atoms that eventually leads to curcumin degradation.

The presence of both cycloamylose and amylopectin clusters in 96 GS may also have significantly increased the UV stability of curcumin. The increased UV stability of curcumin encapsulated with 96 GS may be attributed not only to the complexation effect, but also to the physical barrier caused by amylopectin clusters. According to the Mw distribution and chain length distribution analysis (sec. 3.1.1), 96 GS had a broader chain length distribution and narrower Mw distribution than 1 GS 96 GS was also more likely to complex with iodine, possibly owing to the presence of cycloamylose (sec 3.1.2.). Min et al. (2010) reported that polymers with uniform Mw distribution tended to act as denser and more rigid wall materials, resulting in stronger protective effects. Therefore, we can conclude that the cycloamylose and amylopectin clusters with narrow chain length distribution observed in 96 GS conferred protective complexation effects by hydrogen bonding, while
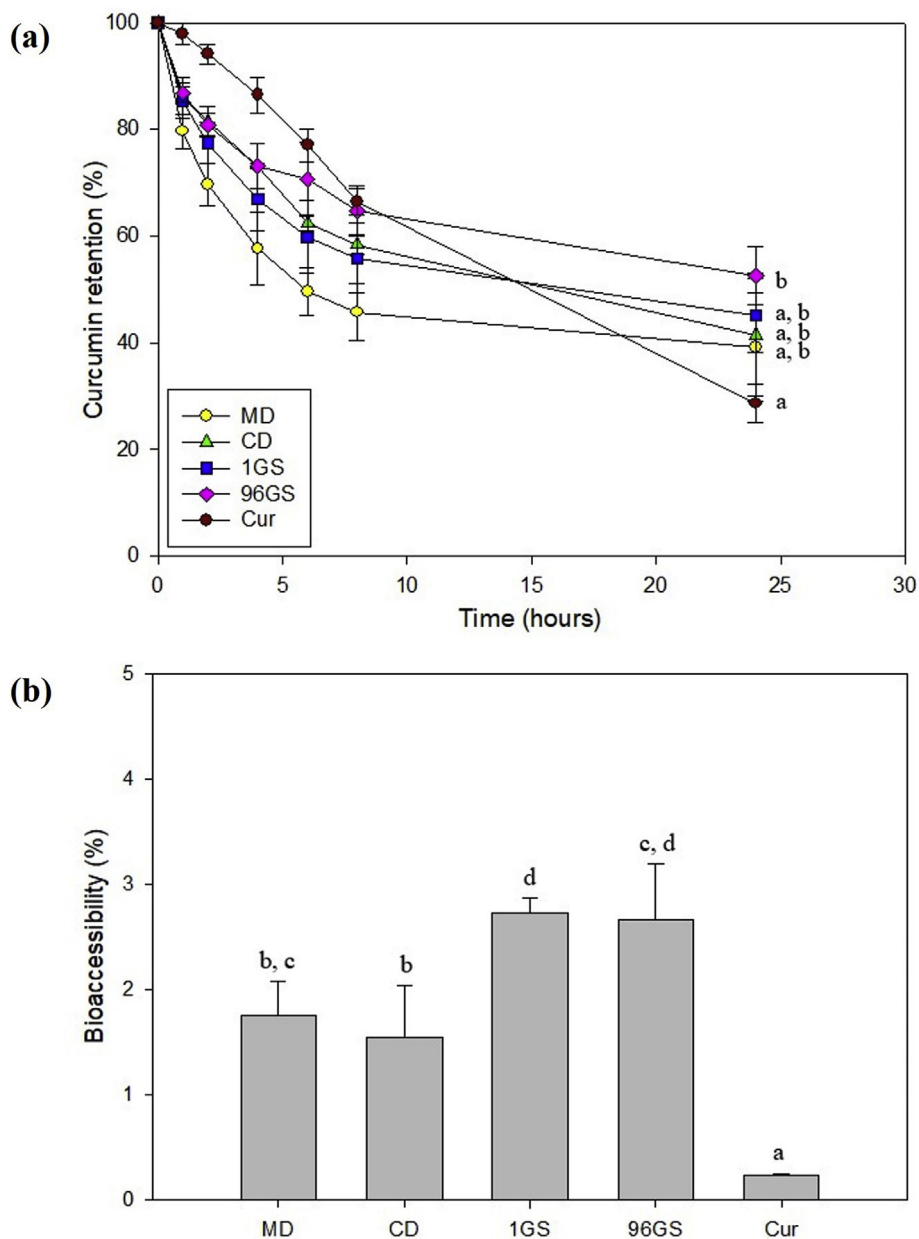
Fig. 5. (a) The % retention of curcumin encapsulated with host materials after UVC exposure for 24 h. (b) Bioaccessibility of curcumin with and without host materials.

the amylopectin clusters further protected curcumin by forming a dense physical barrier. From these results, the increased UV stability of the curcumin encapsulated with 96 GS may extend shelf-life during storage and allow short UV sterilization processes to be exploited.

3.2.4. In vitro bioaccessibility assay

The *in vitro* bioaccessibility of Cur and encapsulated curcumin was examined to determine whether encapsulation provided shielding effects under simulated physiological environmental conditions, such as pH variation and mechanical stirring. Bioaccessibility evaluation has been carried out more frequently using the oil and water (O/W) emulsion system, since lipids are needed to form micelles in the intestinal phase during digestion (Marefati, Bertrand, Sjoo, Dejmek, & Rayner, 2017; Mun, Choi, & Kim, 2015; Mun et al., 2015; Zou, Liu, Liu, Xiao, & McClements, 2015). In the present study, bioaccessibility was measured to examine how the physiological conditions affected the overall solubility and stability of the encapsulated curcumin. To

measure the bioaccessibility of curcumin, Cur and reconstituted curcumin complexes encapsulated with MD, CD, 1 GS and 96 GS (MD-cur, CD-cur, 1 GS-cur, and 96 GS-cur) were treated using a simulated digestion system consisting of oral, stomach and intestinal phases. As shown in Fig. 5b, the 1 GS-cur exhibited significantly higher bioaccessibility (2.73 ± 0.14%) than Cur (0.24 ± 0.01%), MD (1.75 ± 0.32%) and CD (1.55 ± 0.50%) ($p < 0.05$). The 96 GS-cur (2.66 ± 0.52%) exhibited significantly higher bioaccessibility values than CD and Cur. The CD-cur had the lowest bioaccessibility, but it was still significantly higher than that of Cur ($p < 0.05$).

These results are broadly consistent with the results of the pH stability analysis, possibly because the digestive environment involved variations in pH from 2 to 7 As previously discussed (sec. 3.2.3.1), the MD-cur and CD-cur had relatively low pH stability compared to 1 GS-cur and 96 GS-cur under basic conditions, and compared to 1 GS under acidic conditions. Similarly, 1 GS-cur and 96 GS-cur had higher bioaccessibility than CD-cur, MD-cur and Cur. In other words, the increased

bioaccessibility after passing through the digestion system may be related to its increased pH stability of GS-cur. Furthermore, the high bioaccessibility of 96 GS-cur, which showed low stability under acidic pH conditions, may be attributed to the pH-dependent reversibility of 96 GS, as previously suggested (sec. 3.1.3). Given that the aggregation of 96 GS was reversible depending on pH (Fig. 2b), aggregated starch in the stomach phase may have been partly unfolded under basic conditions in the intestinal phase, maintaining curcumin content to some degree.

In addition, the overall low bioaccessibility of this encapsulation system compared to emulsion systems can be explained by the absence of oil. Hydrophobic compounds usually require incorporation into mixed micelles within the small intestine (Mun et al., 2015). However, only simple mixed micelles consisting of bile salts and phospholipids were formed in the absence of lipid digestion products (Madenci & Egelhaaf, 2010). When the complex mixed micelles were incorporated into the O/W emulsion system with beta-carotene, approximately 1–23% of bioaccessibility was achieved, depending on the initial oil content (2–8%) (Mun et al., 2015). Conversely, the present study did not involve any oil, facilitating the production of chemical- and oil-free complexes and reducing the limitations associated with food system applications. Given that the present study did not include oil, the observed bioaccessibility (2.66 and 2.73% for 96 GS and 1 GS, respectively) was high compared to O/W emulsion systems with less than 2% fat content, which resulted in approximately 1% bioaccessibility of beta-carotene in a previous study (Mun et al., 2015). Therefore, the increased bioaccessibility of curcumin in this encapsulation system seems to rely not only on the formation of micelles as O/W emulsion system usually does, but also on the improved pH stability facilitated by GS. However, further research is required to increase bioaccessibility without incorporating fats by altering the starch concentration or ratio of starch to curcumin.

4. Conclusion

The results of the present study suggest that GS improves curcumin water solubility, bioaccessibility and stability under various environmental conditions through simple encapsulation. GS was found to provide stronger shielding effects than MD and CD, which have been used in many previous encapsulation studies. After encapsulation using 96 GS (6% w/v), the solubility of curcumin was about 2,846-fold higher than that of Cur. The UV stability and pH stability of the curcumin encapsulated with GS was significantly enhanced. Even though 96 GS underwent aggregation under acidic pH, it successfully protected curcumin under the physiological condition with its reversible pH-induced aggregation. The encapsulation of curcumin using GS also increased bioaccessibility, possibly through improved pH stability. The shielding effects of GS on curcumin may be attributed to the unique physicochemical properties that arise from 4αGTase treatment, such as Mw distribution, chain length distribution and the coexistence of cyclic glucans and highly branched amylopectin clusters. Therefore, our study shows that 4αGTase-treated starch may be used to encapsulate hydrophobic bioactive compounds, to enhance stability and solubility in food and drug systems.

Acknowledgements

Appendix A. Supplementary data

Supplementary data to this article can be found online at https://doi.org/10.1016/j.foodhyd.2019.04.012.

References

Aboubacar, A., & Hamaker, B. R. (2000). Low molecular weight soluble starch and its relationship with sorghum couscous stickiness. *Journal of Cereal Science, 31*(2), 119–126. https://doi.org/10.1006/jcrs.1999.0262.

Ansari, M. J., & Parveen, R. (2016). Solubility and stability enhancement of curcumin: Improving drug properties of natural pigment. *Drug Development and Therapeutics, 7*(2), https://doi.org/10.4103/2394-6555.191166.

Bailey, J. M., & Whelan, W. J. (1961). Physical Properties of Starch 1. relationship between iodine stain and chain length. *Journal of Biological Chemistry, 236*(4), 969–973.

Biwer, A., Antranikian, G., & Heinzle, E. (2002). Enzymatic production of cyclodextrins. *Applied Microbiology and Biotechnology, 59*(6), 609–617. https://doi.org/10.1007/s00253-002-1057-x.

Brazel, C. S., & Rosen, S. L. (2013). *Fundamental principles of polymeric materials.* Hoboken, N.J: Wiley.

Cho, K.-H., Auh, J.-H., Kim, J.-H., Ryu, J.-H., & Park, K. H. (2009a). Effect of amylose content on corn starch modification by *Thermus aquaticus* 4-α-Glucanotransferase. *Journal of Microbiology and Biotechnology, 19*(10), 1201–1205. https://doi.org/10.4014/jmb.0905.05048.

Cho, K. H., Auh, J. H., Ryu, J. H., Kim, J. H., Park, K. H., Park, C. S., et al. (2009b). Structural modification and characterization of rice starch treated by *Thermus aquaticus* 4-α-glucanotransferase. *Food Hydrocolloids, 23*(8), 2403–2409. https://doi.org/10.1016/j.foodhyd.2009.06.019.

Clerici, M. T. P. S., & Schmiele, M. (2019). *Starches for food application: Chemical, technological and health properties.* London, U.K: Academic Press.

Del Valle, E. M. M. (2004). Cyclodextrins and their uses: A review. *Process Biochemistry, 39*(9), 1033–1046. https://doi.org/10.1016/s0032-9592(03)00258-9.

Do, H. V., Lee, E.-J., Park, J.-H., Park, K.-H., Shim, J.-Y., Mun, S., et al. (2012). Structural and physicochemical properties of starch gels prepared from partially modified starches using *Thermus aquaticus* 4-α-glucanotransferase. *Carbohydrate Polymers, 87*(4), 2455–2463. https://doi.org/10.1016/j.carbpol.2011.11.021.

Esatbeyoglu, T., Huebbe, P., Ernst, I. M., Chin, D., Wagner, A. E., & Rimbach, G. (2012). Curcumin–from molecule to biological function. *Angewandte Chemie International Edition in English, 51*(22), 5308–5332. https://doi.org/10.1002/anie.201107724.

Fennema, O. R., Damodaran, S. E., & Parkin, K. L. (2017). *Food chemistry.* Boca Raton: CRC Press. https://doi.org/10.1201/9781315372914.

Higuchi, T., & Connors, K. A. (1965). Phase solubility techniques. *Advances in Analytical Chemistry and Instrumentation, 4,* 117–212.

Jain, A. S., Date, A. A., Pissurlenkar, R. R., Coutinho, E. C., & Nagarsenker, M. S. (2011). Sulfobutyl ether(7) beta-cyclodextrin (SBE(7) beta-CD) carbamazepine complex: Preparation, characterization, molecular modeling, and evaluation of in vivo antiepileptic activity. *AAPS PharmSciTech, 12*(4), 1163–1175. https://doi.org/10.1208/s12249-011-9685-z.

Jantarat, C., Sirathanarun, P., Ratanapongsai, S., Watcharakan, P., Sunyapong, S., & Wadu, A. (2014). Curcumin-Hydroxypropyl-beta-Cyclodextrin inclusion complex preparation methods: Effect of common solvent evaporation, freeze drying, and pH shift on solubility and stability of curcumin. *Tropical Journal of Pharmaceutical Research, 13*(8), https://doi.org/10.4314/tjpr.v13i8.4.

Kaminaga, Y., Nagatsu, A., Akiyama, T., Sugimoto, N., Yamazaki, T., Maitani, T., et al. (2003). Production of unnatural glucosides of curcumin with drastically enhanced water solubility by cell suspension cultures of Catharanthus roseus. *FEBS Letters, 555*(2), 311–316. https://doi.org/10.1016/s0014-5793(03)01265-1.

Kaper, T., Maarel, V. D., Euverink, G.-J. W., & Dijkhuizen, L. (2004). Exploring and exploiting starch-modifying amylomaltases from thermophiles. *Biochemistry Society Transactions, 32.*

Kaushik, V., & Roos, Y. H. (2007). Limonene encapsulation in freeze-drying of gum Arabic–sucrose–gelatin systems. *Lebensmittel-Wissenschaft und -Technologie- Food Science and Technology, 40*(8), 1381–1391. https://doi.org/10.1016/j.lwt.2006.10.008.

Kearsley, M. W., & Dziedzic, S. Z. (1995). *Handbook of starch hydrolysis products and their derivatives.* London: Blackie Academic & Professionalhttps://doi.org/10.1007/978-1-4615-2159-4_3.

Kharat, M., Du, Z., Zhang, G., & McClements, D. J. (2017). Physical and chemical stability of curcumin in aqueous solutions and emulsions: Impact of pH, temperature, and molecular environment. *Journal of Agricultural and Food Chemistry, 65*(8), 1525–1532. https://doi.org/10.1021/acs.jafc.6b04815.

Kim, Y., Kim, Y.-L., Trinh, K. S., Kim, Y.-R., & Moon, T. W. (2012). Texture properties of rice cakes made of rice flours treated with 4-α-glucanotransferase and their relationship with structural characteristics. *Food Science and Biotechnology, 21*(6), 1707–1714. https://doi.org/10.1007/s10068-012-0227-6.

Kim, Y. L., Mun, S., Park, K. H., Shim, J. Y., & Kim, Y. R. (2013). Physicochemical functionality of 4-alpha-glucanotransferase-treated rice flour in food application. *International Journal of Biological Macromolecules, 60,* 422–426. https://doi.org/10.1016/j.ijbiomac.2013.04.032.

Knutson, C. A. (1999). Evaluation of variations in amylose-iodine absorbance spectra. *Carbohydrate Polymers, 42,* 65–72.

Lee, B. H., Choi, H. A., Kim, M.-R., & Hong, J. (2013). Changes in chemical stability and bioactivities of curcumin by ultraviolet radiation. *Food Science and Biotechnology, 22*(1), 279–282. https://doi.org/10.1007/s10068-013-0038-4.

Li, J., Shin, G. H., Lee, I. W., Chen, X., & Park, H. J. (2016). Soluble starch formulated nanocomposite increases water solubility and stability of curcumin. *Food Hydrocolloids, 56,* 41–49. https://doi.org/10.1016/j.foodhyd.2015.11.024.

Liu, D., Wu, Q., Chen, H., & Chang, P. R. (2009). Transitional properties of starch colloid with particle size reduction from micro- to nanometer. *Journal of Colloid and Interface Science, 339*(1), 117–124. https://doi.org/10.1016/j.jcis.2009.07.035.

Loksuwan, J. (2007). Characteristics of microencapsulated β-carotene formed by spray drying with modified tapioca starch, native tapioca starch and maltodextrin. *Food Hydrocolloids, 21*(5–6), 928–935. https://doi.org/10.1016/j.foodhyd.2006.10.011.

van der Maarel, M. J. E. C., Capron, I., Euverink, G.-J. W., Bos, H. T., Kaper, T., Binnema, D. J., et al. (2005). A novel thermoreversible gelling product made by enzymatic modification of starch. *Starch - Stärke, 57*(10), 465–472. https://doi.org/10.1002/star.200500409.

van der Maarel, M. J., & Leemhuis, H. (2013). Starch modification with microbial alpha-glucanotransferase enzymes. *Carbohydrate Polymers, 93*(1), 116–121. https://doi.org/10.1016/j.carbpol.2012.01.065.

Madenci, D., & Egelhaaf, S. U. (2010). Self-assembly in aqueous bile salt solutions. *Current Opinion in Colloid & Interface Science, 15*(1–2), 109–115. https://doi.org/10.1016/j.cocis.2009.11.010.

Mangolim, C. S., Moriwaki, C., Nogueira, A. C., Sato, F., Baesso, M. L., Neto, A. M., et al. (2014). Curcumin-beta-cyclodextrin inclusion complex: Stability, solubility, characterisation by FT-IR, FT-Raman, X-ray diffraction and photoacoustic spectroscopy, and food application. *Food Chemistry, 153*, 361–370. https://doi.org/10.1016/j.foodchem.2013.12.067.

Marefati, A., Bertrand, M., Sjöö, M., Dejmek, P., & Rayner, M. (2017). Storage and digestion stability of encapsulated curcumin in emulsions based on starch granule Pickering stabilization. *Food Hydrocolloids, 63*, 309–320. https://doi.org/10.1016/j.foodhyd.2016.08.043.

Min, B. C., Kwon, S. Y., Jeon, Y. S., Lee, B., Baek, H. H., & Park, K. (2010). Maltoheptaose and maltooctaose as the superior aroma encapsulating agents. *Food Science and Biotechnology, 19*(6), 1611–1617. https://doi.org/10.1007/s10068-010-0228-2.

Miranda, J. C., Martins, T. E. A., Veiga, F., & Ferraz, H. G. (2011). Cyclodextrins and ternary complexes: Technology to improve solubility of poorly soluble drugs. *Brazilian Journal of Pharmaceutical Sciences, 47*.

Mohan, P. R. K., Sreelakshmi, G., Muraleedharan, C. V., & Joseph, R. (2012). Water soluble complexes of curcumin with cyclodextrins: Characterization by FT-Raman spectroscopy. *Vibrational Spectroscopy, 62*, 77–84. https://doi.org/10.1016/j.vibspec.2012.05.002.

Mondal, S., Ghosh, S., & Moulik, S. P. (2016). Stability of curcumin in different solvent and solution media: UV-visible and steady-state fluorescence spectral study. *Journal of Photochemistry and Photobiology B, 158*, 212–218. https://doi.org/10.1016/j.jphotobiol.2016.03.004.

Mun, S., Choi, Y., & Kim, Y.-R. (2015). Lipase digestibility of the oil phase in a water-in-oil-in-water emulsion. *Food Science and Biotechnology, 24*(2), 513–520. https://doi.org/10.1007/s10068-015-0067-2.

Mun, S., Choi, Y., Shim, J. Y., Park, K. H., & Kim, Y. R. (2011). Effects of enzymatically modified starch on the encapsulation efficiency and stability of water-in-oil-in-water emulsions. *Food Chemistry, 128*(2), 266–275. https://doi.org/10.1016/j.foodchem.2011.03.014.

Mun, S., Kim, Y. R., & McClements, D. J. (2015). Control of beta-carotene bioaccessibility using starch-based filled hydrogels. *Food Chemistry, 173*, 454–461. https://doi.org/10.1016/j.foodchem.2014.10.053.

Oh, E. J., Choi, S. J., Lee, S. J., Kim, C. H., & Moon, T. W. (2008). Modification of granular corn starch with 4-alpha-glucanotransferase from thermotoga maritima: Effects on structural and physical properties. *Journal of Food Science, 73*(3), C158–C166. https://doi.org/10.1111/j.1750-3841.2007.00655.x.

Pan, M.-H., Huang, T.-M., & Lin, J.-K. (1999). Biotransformation of curcumin through reduction and glucuronidation in mice. *Drug Metabolism and Disposition, 27*(1), 486–494.

Pan, K., Zhong, Q., & Baek, S. J. (2013). Enhanced dispersibility and bioactivity of curcumin by encapsulation in casein nanocapsules. *Journal of Agricultural and Food Chemistry, 61*(25), 6036–6043. https://doi.org/10.1021/jf400752a.

Paramera, E. I., Konteles, S. J., & Karathanos, V. T. (2011). Stability and release properties of curcumin encapsulated in Saccharomyces cerevisiae, β-cyclodextrin and modified starch. *Food Chemistry, 125*(3), 913–922. https://doi.org/10.1016/j.foodchem.2010.09.071.

Park, J.-H., Kim, H.-J., Kim, Y.-H., Cha, H., Kim, Y.-W., Kim, T.-J., ... Park, K.-H. (2007a). The action mode of *Thermus aquaticus* YT-1 4-α-glucanotransferase and its chimeric enzymes introduced with starch-binding domain on amylose and amylopectin. *Carbohydrate Polymers, 67*(2), 164–173. https://doi.org/10.1016/j.carbpol.2006.05.018.

Park, J., Park, K., & Jane, J. (2007b). Physicochemical properties of enzymatically modified maize starch using 4-α-Glucanotransferase. *Food Science and Biotechnology, 16*(6), 902–909.

Perera, C., & Hoover, R. (1999). Influence of hydroxypropylation on retrogradation properties of native, defatted and heat-moisture treated potato starches. *Food Chemistry, 64*, 361–375.

Rachmawati, H., Edityaningrum, C. A., & Mauludin, R. (2013). Molecular inclusion complex of curcumin-beta-cyclodextrin nanoparticle to enhance curcumin skin permeability from hydrophilic matrix gel. *AAPS PharmSciTech, 14*(4), 1303–1312. https://doi.org/10.1208/s12249-013-0023-5.

Sarkar, A., Goh, K. K. T., Singh, R. P., & Singh, H. (2009). Behaviour of an oil-in-water emulsion stabilized by β-lactoglobulin in an in vitro gastric model. *Food Hydrocolloids, 23*(6), 1563–1569. https://doi.org/10.1016/j.foodhyd.2008.10.014.

Shen, X., Bertoft, E., Zhang, G., & Hamaker, B. R. (2013). Iodine binding to explore the conformational state of internal chains of amylopectin. *Carbohydrate Polymers, 98*(1), 778–783. https://doi.org/10.1016/j.carbpol.2013.06.050.

Takaha, T., & Smith, S. M. (1999). The functions of 4-α-glucanotransferases and their use for the production of cyclic glucans. *Biotechnology & Genetic Engineering Reviews, 16*, 257–280.

Takaha, T., Yanase, M., Takata, H., Okada, S., & Smith, S. M. (1996). Potato D-enzyme catalyzes the cyclization of amylose to produce cycloamylose, a novel cyclic glucan. *Journal of Biological Chemistry, 271*, 2902–2908.

Tomono, K., Mugishima, A., Suzuki, T., Goto, H., Ueda, H., Nagai, T., et al. (2002). Interaction between cycloamylose and various drugs. *Journal of Inclusion Phenomena and Macrocyclic Chemistry, 44*, 267–270.

Tonnesen, H. H., Masson, M., & Loftsson, T. (2002). Studies of curcumin and curcuminoids. XXVII. Cyclodextrin complexation: Solubility, chemical and photochemical stability. *International Journal of Pharmaceutics, 244*, 127–135.

Yu, H., & Huang, Q. (2010). Enhanced in vitro anti-cancer activity of curcumin encapsulated in hydrophobically modified starch. *Food Chemistry, 119*(2), 669–674. https://doi.org/10.1016/j.foodchem.2009.07.018.

Zou, L., Liu, W., Liu, C., Xiao, H., & McClements, D. J. (2015). Designing excipient emulsions to increase nutraceutical bioavailability: Emulsifier type influences curcumin stability and bioaccessibility by altering gastrointestinal fate. *Food Function, 6*(8), 2475–2486. https://doi.org/10.1039/c5fo00606f.